AGU PUBLICATIONS

JGR

Journal of Geophysical Research: Space Physics

RESEARCH ARTICLE

10.1002/2017JA024590

Key Points:

- In the plasmasphere boundary layer (PBL) the plasma density N is decreasing exponentially with L
- The width of PBL is proportional to the volume of the unit magnetic flux tube
- Empirical relation describes the dependence of the PBL width on the last K_P burst and on the time delay from the K_P burst

Correspondence to:
G. Kotova and V. Pierrard,
kotova@iki.rssi.ru;
viviane.pierrard@aeronomie.be

Citation:
Kotova, G., Verigin, M., Lemaire, J., Pierrard, V., Bezrukikh, V., & Smilauer, J. (2018). Experimental study of the plasmasphere boundary layer using *MAGION 5* data. *Journal of Geophysical Research: Space Physics*, *123*, 1251–1259. https://doi.org/10.1002/2017JA024590

Received 13 JUL 2017
Accepted 31 JAN 2018
Accepted article online 8 FEB 2018
Published online 20 FEB 2018

Experimental Study of the Plasmasphere Boundary Layer Using *MAGION 5* Data

G. Kotova[1], M. Verigin[1], J. Lemaire[2,3], V. Pierrard[2,3], V. Bezrukikh[1], and J. Smilauer[4]

[1]Space Research Institute of RAS, Moscow, Russia, [2]Université Catholique de Louvain, ELI-C, TECLIM, Louvain-la-Neuve, Belgium, [3]Royal Belgian Institute for Space Aeronomy, Space Physics, Brussels, Belgium, [4]Institute of Atmosphere Physics, Czech Academy of Sciences, Prague, Czech Republic

Abstract The in situ cold plasma measurements onboard *MAGION 5* were carried out with very good time resolution, and this permitted to analyze thin plasmasphere boundary layer (PBL) near the plasmapause. In this layer the plasma density N is decreasing exponentially with L: N~exp(($L_{PP} - L$)/W_B), where W_B corresponds to the characteristic width of the PBL, the distance in L within which the density varies by a factor of e, and L_{PP} is the position of the plasmapause. The density in the boundary layer is inversely proportional to the volume of the unit magnetic flux tube, whereas its width is proportional to the volume of magnetic flux tube. The characteristic width of the PBL linearly depends on the time elapsed since the most recent maximum value of K_P. Empirical relation for the dependence of the PBL width on most recent maximum value of K_P and on the lapse time between this maximum and the plasmapause observations is proposed.

1. Introduction

Different mechanisms have been proposed to explain the formation of the plasmapause (Lemaire & Pierrard, 2008; for a review). Its position is clearly due to the interplay between the electric field associated with the Earth's corotation and the convection electric field associated to geomagnetic activity. The mechanism of interchange instability allows explaining the formation of the sharp density gradient in the postmidnight sector where the electric field is the strongest. When the geomagnetic activity increases during a geomagnetic storm or substorm, the plasmasphere is eroded and a new plasmapause is formed closer to the Earth in this postmidnight sector, as it can be simulated with the three-dimensional dynamic plasmasphere model based on these physical processes (Pierrard & Stegen, 2008). After the storm, the reduced density region refills from ionospheric outflow (Pierrard & Voiculescu, 2011).

Recent spacecraft missions have helped to improve our understanding of the plasmasphere, especially the four *CLUSTER* spacecraft launched in 2000 and still active presently, and Imager for Magnetopause-to-Aurora Global Exploration (*IMAGE*) for which the instrument extreme ultraviolet (EUV) provided from 2000 to 2006 the first global images of the plasmasphere in the equatorial plane when the spacecraft was above the North Pole (Darrouzet et al., 2009; for a review). These images allowed magnetic local time (MLT) analyses of the plasmapause evolution with time (Pierrard & Cabrera, 2006). More recently, the first global meridian images of the plasmasphere were obtained with TEX instrument on board the Japanese *KAGUYA* spacecraft and provided useful information on physical processes of plasmapause formation, confirming the importance of interchange instability mechanism (Murakami et al., 2016). Observations from the Combined Release and Radiation Effects Satellite, *CLUSTER*, and recent the Time History of Events and Macroscale Interactions during Substorms missions also confirm the formation of the plasmapause in the postmidnight sector and its propagation in MLT (Bandic et al., 2016, 2017; Verbanac et al., 2015).

Even if the global dynamics of the plasmasphere is well understood, some questions remain open, including the formation and physical properties of the plasmasphere boundary layer (PBL).

The term PBL was first introduced by Lemaire et al. (1998, p.70) and in more detail by Carpenter and Lemaire (2004). Earlier this layer was called the plasmapause segment by Carpenter and Anderson (1992). The PBL is adjacent to the plasmapause outside of the plasmasphere and can be very thin less than 0.1 R_E (R_E is the Earth's radius) or thick up to 1.5 R_E. The study of this layer is very important for understanding of the physics of energetic particle interactions with the cold magnetospheric plasma as well as the propagation of very low frequency and ultralow frequency waves into the magnetosphere.

Plasmasphere boundary layer is consistent with density gradients observed in the ionosphere where special phenomena are observed such as polarization jet (elsewise named subauroral ion drifts or subauroral polarization stream) (Khalipov et al., 2016), stable midlatitude red arcs (Mendillo et al., 2016), and subauroral morning proton spots (Frey et al., 2004). The density distribution in the PBL is also important in modulating ultralow frequency waves observed in space and on the ground (Liu et al., 2013; Moldwin & Zou, 2012). Despite all these related phenomena, not much attention was paid, so far, to the experimental and theoretical description of PBL properties and mechanism of its formation.

Kotova et al. (2017) analyzed cold plasma data, obtained by *INTERBALL 1*. They estimated the width of the PBL as a difference between plasmapause positions determined using two alternative empirical methods. The plasmapause position was determined from density versus L profiles as suggested by Carpenter and Anderson (1992) and otherwise from the sequence of measured spectra of cold ions. The authors estimated the average plasmapause width in the equatorial plane to be 0.4–0.5 R_E and the maximum width to be 1.4 R_E.

Plasma density structures close to the plasmapause were observed by Décréau et al. (2005) using data from the WHISPER experiment onboard of *CLUSTER*. In their statistical study, the characteristic dimensions of small-scale field aligned and cross-field plasma structures have been analyzed, as well as their dynamical changes.

This paper uses in situ cold plasma measurements obtained with a high time resolution instrument on-board *MAGION 5*. This permitted to analyze the rather thin boundary layers outside the plasmapause and to identify some general features of the PBL.

2. Experimental Data

The Czech subsatellite *MAGION 5* was launched in August 1996, together with the main *INTERBALL-2* spacecraft, into an orbit with inclination of ~65°, orbit perigee of ~1.2 R_E, and apogee of ~4 R_E. Unfortunately, after 1 day of operation, the communication with the subsatellite was lost. It was restored only in 20 months after launch. Fortunately, after recovery, all spacecraft systems operated normally. *MAGION-5* carried the plasma analyzer with retarding potential PL-48, observing the thermal plasma in the Earth's plasmasphere. Data were collected since August 1999, when the instrument carrying bar was deployed, till July 2001, when the satellite's service came to an end. The time to measure one energy spectrum of the cold protons was 0.4 s, and this was repeated every ~8 s (Kotova et al., 2008).

With a nearly 6 hr orbital period the plasmasphere was crossed 4 times per day, but for various programmatic reasons, in most of cases, the data are available only during one descending leg of the orbit per day. The data processing technique is described by Kotova et al. (2014).

For this analysis of the PBL, we scanned through all proton density profiles $N(L)$ versus McIlwain's L-parameter, available from the *MAGION 5* mission. We selected 110 profiles of relatively smooth, nonstructured boundary layers.

Figure 1 shows two examples of $N(L)$ profiles without clear boundary layer observations (Figures 1a and 1b) as well as two others with well-developed PBL (Figures 1c and 1d).

In all cases the density in the PBL is well described by the straight line in coordinates ($\ln N$, L), that is, $N(L) = N_{PP} \times \exp((L_{PP} - L)/W_B)$, where N_{PP} is the proton density at the plasmapause L_{PP}, and where W_B corresponds to the characteristic width of the PBL, that is, the distance in L within which the density decreases by a factor of e. Following Carpenter and Anderson (1992), the equatorial position of the plasmapause L_{PP}—originally called Carpenter's "knee"—is determined as the position of the last measured point prior to the sharp density drop by a factor of 5 or more within half an Earth's radius. Using the *INTERBALL-1* data, Kotova et al. (2017) found that the observed values of L_{PP} correspond rather satisfactorily with "best fitted positions" of their 3-D semiempirical model of the plasmapause. The latter 6-parametric semiempirical model was already used in an earlier study by Kotova et al. (2015).

3. Properties of the Plasmasphere Boundary Layer

Let us first examine the density inside the boundary layer as a function of the equatorial distance of the PBL. The volume per unit magnetic flux of a tube of plasma is given by the expression (Khazanov, 2011):

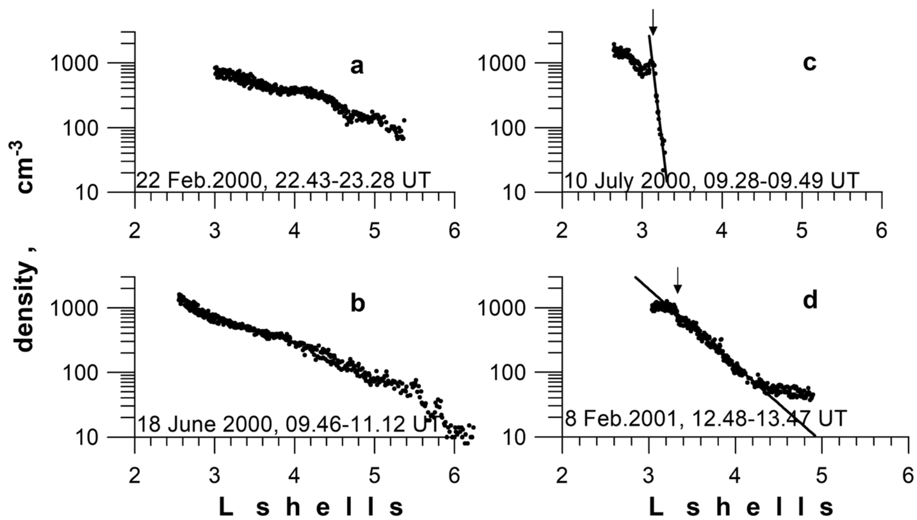

Figure 1. (a–d) Examples of cold plasma density distribution along the orbits of MAGION 5 as a function of L. The solid lines in c and d represent the dependence $N(L) = N_{PP} \times \exp((L_{PP} - L)/W_B)$. The arrows mark the position of the plasmapause.

$$\mathrm{Vol}(L) = \frac{L^4}{a}\cdot\sqrt{1-\frac{1}{L}}\cdot\left(1+\frac{1}{2L}+\frac{3}{8L^2}+\frac{5}{16L^3}\right), \quad (1)$$

where $a = 35B_E/32R_E$, and where B_E is the magnetic field on the surface of the Earth at the equator (a derivation process is given in Appendix A).

Figure 2 shows the dependence of the cold plasma density $N(L_{PP} + W_B)$ in the boundary layer on the volume per unit magnetic flux of a tube of plasma at $L = (L_{PP} + W_B)$ shell. The solid line in Figure 2 is a fit of $N(L_{PP} + W_B)$ by the mathematical expression $28{,}300/(a \cdot \mathrm{Vol}(L_{PP} + W_B))$.

It can be seen that the density inside the boundary layer at $L = (L_{PP} + W_B)$ is inversely proportional to the volume of the unit magnetic flux tube. This implies that N_T, the total plasma content of the unit flux tube, tends to be nearly constant in the PBL at $L = (L_{PP} + W_B)$. This property of the PBL may be of key importance, since it can permit to check the validity of future theories for the formation of the PBL. Note that this statistical results over an ensemble of PBL, but it does not imply that the total plasma content in unit magnetic flux tubes, $N_T(L)$, is necessarily independent of L within each individual PBL.

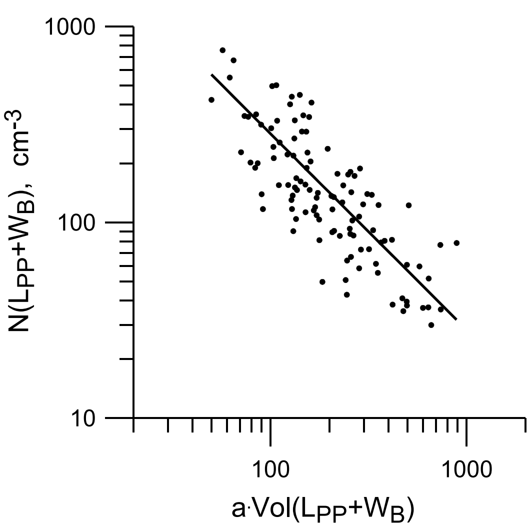

Figure 2. Cold plasma density inside the plasmasphere boundary layer versus the volume per unit magnetic flux of a tube of plasma. The solid line denotes the fitting dependence $28{,}300/(a \cdot \mathrm{Vol}(L_{PP} + W_B))$.

Another interesting statistical property of the PBLs is the dependence of their widths, W_B, on the equatorial distance L_{PP}. Figure 3 shows the distribution of $W_B(L_{PP})$ for all 110 PBL crossings. This statistical distribution can be fitted by the solid curve which corresponds to the fit function $0.00043 \cdot a \cdot \mathrm{Vol}(L_{PP})$. This indicates that the average characteristic width of the PBL is statistically proportional to the volume of the unit flux tube at L_{PP}.

It is intuitively clear that the PBL width should be lower after higher Kp burst. It also seems clear that the longer time has passed since the burst of Kp, the wider PBL should be observed. Next, we check these suppositions and analyze the influence of geomagnetic activity on the equatorial position of the PBL, as well as the dependence of W_B on the time elapsed since the last peak of the K_P index.

It is well known that the equatorial position of the plasmapause is a linear function of the geomagnetic activity index K_P (Carpenter & Anderson, 1992; Pierrard et al., 2009, for a review). The popular relationship which was published by Carpenter and Anderson (1992) is given

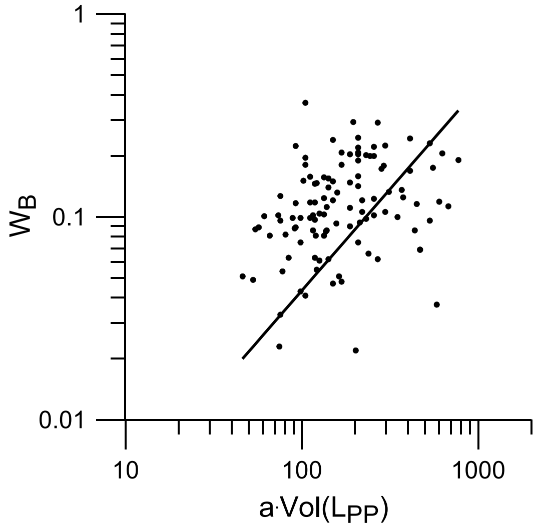

Figure 3. Dependence of the plasmasphere boundary layer characteristic width on the volume per unit magnetic flux of a tube of plasma. The solid line shows the fitting by relation (1).

by L_{PP} = 5.6–0.46$K_{P\max}$, where $K_{P\max}$ is the maximum 3 hourly K_P index during the 24 hr preceding the time of the observation of the plasmapause. In our study, using the *MAGION 5* data, we have checked a longer time interval of 48 hr but considered the last peak value of K_P with $K_P \geq 3$ preceding the plasmapause measurements which sometimes may occur either earlier or later than observation of the maximum K_P index during the 24 hr prior the plasmapause observation. In case we could not find any K_P peak higher than 3, we checked the data again and chose any peak value of K_P closest to the time of plasmapause observation. This value of K_P will be designed by the symbol K_{PB}. This K_P burst or peak is sometimes accompanied by the main phase decrease of the *Dst* index. A longer time interval is adopted since significant geomagnetic disturbances change plasmasphere characteristics for a period of more than 24 hr. Figure 4 illustrates the value of K_{PB} for the observations of 8 February 2001 shown in Figure 1d. We introduce also the symbol Δt_{Kp} to denote the lapse time between the *MAGION-5* observations, and the time of the last peak value of K_P (K_{PB}), as described above.

Figure 5 shows the equatorial position of the plasmapause for the selected 110 cases versus K_{PB}. The solid line in the figure shows the relationship of Carpenter and Anderson (1992), where $K_{P\max}$ has been replaced by K_{PB}. Despite the difference in the selection of K_P the good correspondence between *MAGION* 5 plasmapause observations and the linear function L_{PP} = 5.6–0.46K_{PB} is obvious and must be pointed out.

Figure 6 shows W_B as a function of K_{PB} for Δt_{Kp} less than 12 hr. This figure shows that the width of the boundary layer decreases when K_{PB} increases. This nonlinear dependence can be obtained by the combining the relationships shown in Figures 3 and 5. The resulting relationship corresponds to the solid line in Figure 6:

$$W_B = b{\cdot}a{\cdot}\mathrm{Vol}(L_{PP}) = b{\cdot}a{\cdot}\mathrm{Vol}(5.6\text{–}0.46\ K_{PB}) \qquad (2)$$

with b = 0.00044. Fitting of the observed values of W_B displayed in Figure 6 to the function Vol(5.6–0.46 K_{PB}) gives the coefficient b = 0.00042, which is almost identical to that obtained from the relationships $W_B(L_{PP})$ and $L_{PP}(K_{PB})$.

Therefore, it can be concluded that dependence of W_B on K_{PB} discovered in this study is a straightforward consequence of the relationships between the plasmapause position and K_{PB} and between W_B and L_{PP}.

It was suggested above that W_B, the width of the PBL, depends also on Δt_{Kp}, the lapse time between the plasmapause and K_{PB} observations. Despite the large scatter of the points shown in Figure 7, it can be seen that W_B depends on the lapse time Δt_{Kp}. When Δt_{Kp} is equal to 9 hr or more, Figure 7 suggests the existence of a linear relationship between $\boldsymbol{W_B}$ and the lapse time:

$$W_B = 0.0061 \times \Delta t_{Kp} + 0.047 \qquad (3)$$

The data corresponding to values of Δt_{Kp} smaller than 9 hr have been excluded from this figure due to their large scatter leading to the underestimation of the slope of the fitting line. The increasing scatter for values of the time lapse smaller than 9 hr may be explained by the low time resolution of the *Kp* index; indeed, the latter is equal to 3 hr.

Thus, it can be concluded that the width of PBL is indeed a function of at least both variables K_{PB} and Δt_{Kp}. For small lapse times W_B depends mostly on K_{PB} (see equation (2)), while for lapse times larger than 9 hr, the PBL width depends linearly on this lapse (see equation (3)).

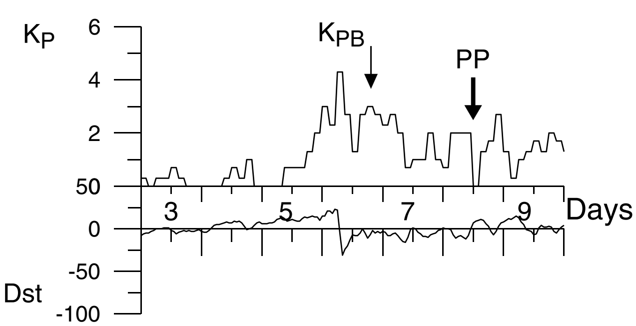

Figure 4. K_P and *Dst* variations on 3–9 February 2001. The bold arrow marks the time of the plasmapause crossing (PP) by *MAGION-5*, and the thin arrow marks the K_{PB} position.

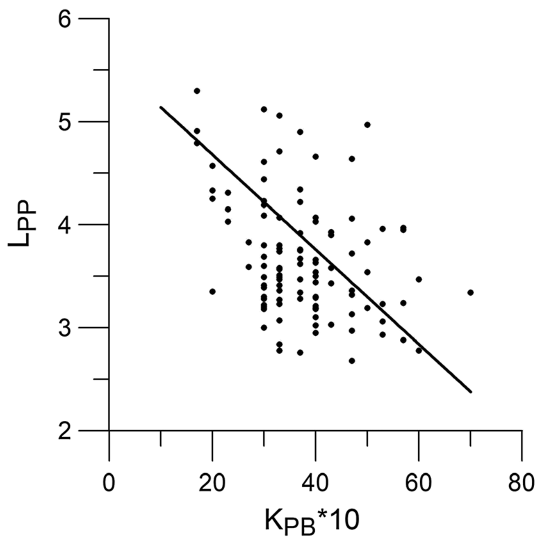

Figure 5. Dependence of the plasmapause position on the K_P burst prior to the plasmapause observation. The solid line shows the function L_{PP} = 5.6–0.46K_{PB}.

To describe the PBL width within the whole interval of the lapse times for all the 110 experimental points, the combination of the relations (2)) and (3)) can be used:

$$W_{BCalc} = C \cdot \Delta t_{Kp} + D \cdot a \cdot \mathrm{Vol}(5.6–0.46\ K_{PB}) \tag{4}$$

Coefficients C and D can be determined by minimization of the sum S of square differences between the experimental PBL widths and widths calculated with expression (4):

$$S = S(W_B - W_{BCalc})^2 \\ C = 0.0045, \quad D = 0.000366 \tag{5}$$

The comparison of experimental and calculated widths of PBL is presented in Figure 8. On the solid line $W_B = W_{BCalc}$. It is seen that the relation (4) well describes the experimental data and can be used for the estimation of the average width of the PBL.

It is worth mentioning that no dependence of $\boldsymbol{W_B}$ on MLT was found except that indirectly involved in Δt_{Kp}. This fact is likely connected with the distribution of selected PBL observations by MLT. While there were PBL observations in all MLT sectors, the most number of cases is referred to the dawn-afternoon sector, and thus, MLT dependence of PBL characteristics cannot be analyzed reliably with the considered set of data.

4. Discussion and Conclusion

In situ cold plasma measurements obtained with a high time resolution instrument on-board *MAGION 5* were used to analyze physical properties of the PBL.

Previously *MAGION 5* data were used for the in situ study of notch structures in the plasmasphere (Kotova et al., 2008). These structures were first observed by the EUV Imager on board the *IMAGE* spacecraft. In this study, selected plasmapause positions determined by *MAGION 5* were compared with EUV/*IMAGE* images (Figure 4 in Kotova et al., 2008). It was shown that the plasmapause position determined by the *MAGION 5* data well agrees with the *IMAGE* spacecraft observations.

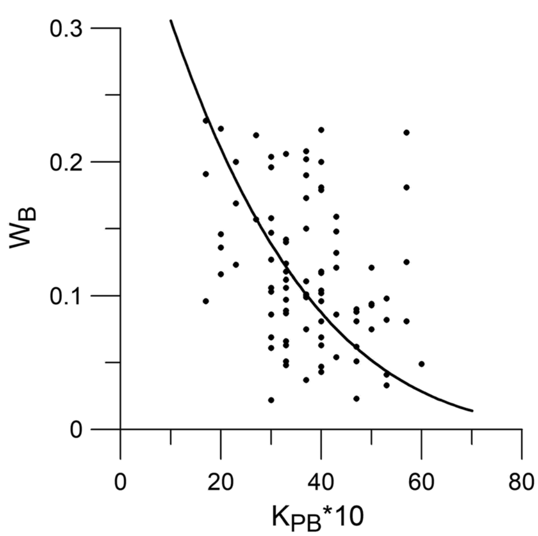

Figure 6. Dependence of the plasmasphere boundary layer characteristic width on the K_{PB} index for $\Delta t_{Kp} < 12$ hr. The solid line shows the function $\boldsymbol{W_B}$ = 0.00044 · a · Vol(5.6–0.46K_{PB}).

A series of 110 proton density profiles $N(L)$ observed by the *MAGION 5* satellite have been analyzed. The density distribution used in this study corresponds to relatively quiet PBLs without large amplitude structures. In all cases selected here, the density distribution in the boundary layer is rather well described by a linear dependence in ln$N$-L coordinates. From the present statistical study, a number of general physical properties of PBL have been obtained.

- The density in the PBL at $L = (L_{PP} + W_B)$ is statistically proportional to the inverse of the volume of unit magnetic flux tube at this distance as given by equation (1). As a consequence, N_T, the total plasma content of the unit flux tube at $L = (L_{PP} + W_B)$ tends to be nearly constant in the PBL.
- The characteristic width of the PBL, W_B, depends on L_{PP}, the equatorial distance of the plasmapause, and is proportional to the volume of the unit magnetic flux tube at this same distance.
- The characteristic width of the PBL, W_B, is a linear function of Δt_{Kp}, the time elapsed since the most recent peak (burst) of the value of K_P (equation (3)).
- The value of W_B is also a function of K_{PB}, the maximum value of K_P at the earlier time (see equation (2)). This dependence of W_B on K_P is described through (i) the volume of the unit magnetic flux tube

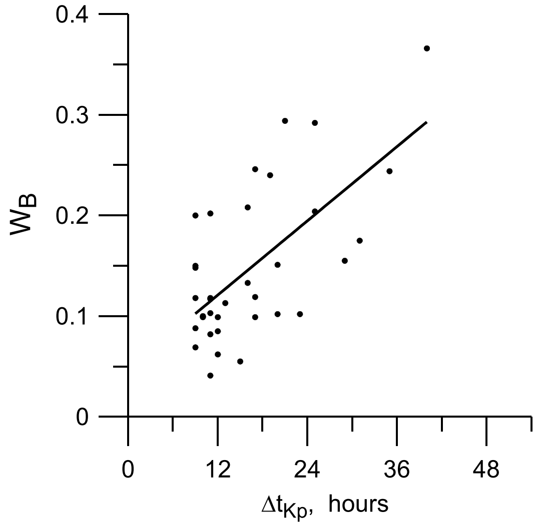

Figure 7. Dependence of W_B on the time elapsed since the most recent maximum value of K_P, for $\Delta t_{Kp} > 9$ hr. The solid line is a linear fitting $W_B = 0.0061.\Delta t_{Kp} + 0.047$.

given by equation (1) and (ii) the empirical relationship between L_{PP} and K_{PB}, which is similar to that derived by Carpenter and Anderson (1992).

- An empirical relationship between W_B (i) and K_{PB}, the most recent peak of K_P as determined in section 3, and (ii) Δt_{Kp}, the lapse time since the most recent peak of K_P, has been deduced. It is given by equation (4).

The last property supports the intuitive expectation that the PBL width should be lower after higher *Kp* burst and that the longer time has passed after the burst of *Kp*, the wider PBL will be observed.

The most unexpected property in this list is the second one. It awaits a satisfactory physical explanation that is not yet available. It is likely related to refilling process for which many problems remain unsolved (Gallagher & Comfort, 2016).

The last three properties give us some hint on the mechanism of formation of PBL. Indeed, the second term in equation (4) corresponds to the initial characteristic width of the PBL—the distance in *L* within which the density decreases by a factor of *e*—at the epoch of formation of a new plasmapause, that is, at the time of the most recent K_P burst. For sufficiently large K_{PB} (>~5) this initial characteristic width W_B is ~$0.04R_E$ in the equatorial plane. This corresponds to the *L*-range of about 0.1 R_E over which the equatorial density decreases by a factor 10, as found in the plasmapause "segment" by Carpenter and Anderson (1992) from the Sweep Frequency Receiver observations collected on board of the ISEE-1 satellite.

From Figure 7 it can be seen that W_{bmax}, the maximum characteristic width of PBL, is ~0.4 R_E, according to the *MAGION-5* data examined in this study.

The first term in equations (3) and (4) determines the rate of the change of the PBL width, which connected with the rate of refilling of magnetic flux tubes depleted during peeling off events of the plasmasphere. The time required to recover an almost saturated plasmasphere can thus be determined from equations (3) and (4). The latter is only about 3 days, which is significantly smaller than the time needed to reach diffusive equilibrium in dipole magnetic flux tubes. This confirms that diffusive equilibrium is almost never obtained in the plasmasphere or in the plasmatrough. The continual radial plasmaspheric wind predicted by Lemaire and Schunk (1992, 1994) and detected by Dandouras (2013) is evidently the reason for apparent discrepancy between the actual refilling time and that required to reach diffusive equilibrium in the plasmasphere. This difference is well known since the pioneering whistler observations by Park (1973) and Tarcsai (1985).

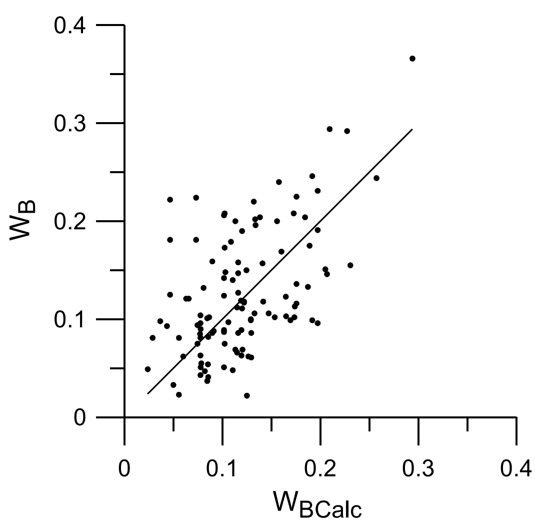

Figure 8. Comparison of experimental and calculated widths of plasmasphere boundary layer. On the solid line $W_B = W_{BCalc}$.

The first generation of magnetohydrodynamic (MHD) models proposed for the formation of the Plasmapause was based on the last closed equipotential scenario. It was first proposed by Nishida (1966) and subsequently by Brice (1967). It was based on the assumption of an ad-hoc steady state magnetospheric electric field model. Other MHD models for the formation of the plasmapause have been proposed subsequently by Chen and Wolf (1972). These latter geometrical models were based on tedious calculations of last closed streamlines; they were also fitted by ad-hoc *Kp*-dependent empirical models for the magnetospheric electric field distribution.

Unfortunately so far, no comprehensive model for the variable magnetospheric *E*-field distribution has yet been determined from direct observations, unlike for the geomagnetic field (International Geomagnetic Reference Field; Tsyganenko and Sitnov, 2007). Therefore, none of the past MHD scenarios, nor existing kinetic simulation based on the quasi-interchange mechanism, can be considered with enough confidence as adequate predictions of the actual positions and shapes of the plasmapause as determined from ground based whistler observations or from in situ spacecraft measurements. The PBL can be formed as a consequence of quasi-interchange plasma motion becoming convectively unstable beyond the zero-parallel-force surface introduced by Lemaire (1974, 1976, 1985) and comprehensively modeled by André (2003) as part of his PhD thesis (see also André & Lemaire, 2006). Lemaire's interchange mechanism also well describes the position and formation of the plasmapause "knee," instead the former last closed equipotential and last closed streamline scenarios (see also Lemaire & Kowalkowski, 1981). From Lemaire and Pierrard's (2008) simulations, it has been possible to infer that the computed values of L_{PP} fit more closely those determined from the IMAGE/EUV observations.

But, of course, this expectation needs to be confirmed by future theoretical studies and numerical simulations which are beyond the scope of our first statistical study of the PBL.

Appendix A

At distances not far from the Earth the geomagnetic field can be approximated by a dipole field (e.g., Baumjohann & Treumann, 1997):

$$B(r,\lambda) = \frac{B_E R_E^3}{r^3} \cdot \sqrt{1 + 3\sin^2\lambda} \tag{A1}$$

The dipole field line equation is

$$r = R_E L \cdot \cos^2\lambda \tag{A2}$$

where λ is magnetic latitude. The element of arc-length along a field line is given by

$$dl = \sqrt{(dr)^2 + r^2 \cdot (d\lambda)^2}, \tag{A3}$$

and the volume element of a flux tube is $dV = dl \cdot ds$, where ds is the cross-sectional area of the flux tube. If B is magnetic field value along a field line, the magnetic flux of a tube of plasma through the cross-sectional area ds is $B \cdot ds$. Then the volume per unit magnetic flux of a tube of plasma is given by

$$\mathrm{Vol}(L) = \int \frac{dl}{B} = \int \frac{dl}{d\lambda} \cdot \frac{d\lambda}{B}. \tag{A4}$$

From equations (A2) and (A3), it follows that

$$\frac{dl}{d\lambda} = R_E L \cdot \cos\lambda \cdot \sqrt{1 + 3\sin^2\lambda}. \tag{A5}$$

Taking into account equation (A2), expression (A1) can be rewritten as

$$B(L,\lambda) = \frac{B_E}{L^3} \cdot \frac{\sqrt{1 + 3\sin^2\lambda}}{\cos^6\lambda} \tag{A6}$$

The integral (A3) is taken from the surface of the Earth in one hemisphere to the surface of the Earth in another hemisphere; this means the integral from $\lambda = -\Lambda_0 = \arccos\sqrt{1/L}$ to $\lambda = \Lambda_0$. Substituting expressions (A5) and (A6) into (A4), one can obtain the volume per unit magnetic flux:

$$\mathrm{Vol}(L) = \frac{32}{35} \frac{L^4 R_E}{B_E} \cdot \sqrt{1 - \frac{1}{L}} \cdot \left(1 + \frac{1}{2L} + \frac{3}{8L^2} + \frac{5}{16L^3}\right). \tag{A7}$$

Acknowledgments
The authors thank the Solar-Terrestrial Center of Excellence and the interuniversity project CHARM for their support. The data of PL48/MAGION 5 are now available on the website of the Space Research Institute of RAS http://www.iki.rssi.ru/interball/magion5/ and upon request to J. Šmilauer, the principal investigator of the experiment, jsm@ufa.cas.cz, and/or G. Kotova, kotova@iki.rssi.ru.

References

André, N. (2003). Ondes et instabilités basse-fréquence dans un plasma gyrotrope. Application à l'instabilité d'interchange dans les magnétosphères des planètes géantes, (PhD thesis). Université Paul Sabatier.

André, N., & Lemaire, J. F. (2006). Convective instabilities in the plasmasphere. *Journal of Atmospheric and Solar: Terrestrial Physics*, *68*, 213–227.

Bandic, M., Verbanac, G., Moldwin, M., Pierrard, V., & Piredda, G. (2016). MLT dependence in the relationship between plasmapause, solar wind and geomagnetic activity based on CRRES: 1990–1991. *Journal of Geophysical Research: Space Physics*, *121*, 4397–4408. https://doi.org/10.1002/2015JA022278

Bandic, M., Verbanac, G., Pierrard, V., & Cho, J. (2017). Evidence of MLT propagation of the plasmapause inferred from THEMIS data. *Journal of Atmospheric and Solar: Terrestrial Physics*, *161*, 55–63. https://doi.org/10.1016/j.jastp.2017.05.005

Baumjohann, W., & Treumann, R. A. (1997). *Basic space plasma physics* (p. 329). London: Imperial College Press.
Brice, N. M. (1967). Bulk motion of the magnetosphere. *Journal of Geophysical Research*, *72*(21), 5193–5211. https://doi.org/10.1029/JZ072i021p05193
Carpenter, D. L., & Anderson, R. R. (1992). An ISEE/whistler model of equatorial electron density in the magnetosphere. *Journal of Geophysical Research*, *97*(A2), 1097–1108. https://doi.org/10.1029/91JA01548
Carpenter, D., & Lemaire, J. (2004). The plasmasphere boundary layer. *Annales de Geophysique*, *22*(12), 4291–4298. https://doi.org/10.5194/angeo-22-4291-2004
Chen, A. J., & Wolf, R. A. (1972). Effects on the plasmasphere of time-varying convection electric field. *Planetary and Space Science*, *20*(4), 483–509. https://doi.org/10.1016/0032-0633(72)90080-3
Dandouras, I. (2013). Detection of a plasmaspheric wind in the Earth's magnetosphere by the Cluster spacecraft. *Annales de Geophysique*, *31*(7), 1143–1153. https://doi.org/10.5194/angeo-31-1143-2013
Darrouzet, F., De Keyser, J., & Pierrard, V. (Eds.) (2009). *The Earth's plasmasphere: A cluster and IMAGE perspective* (p. 296). Brussels: Springer. https://doi.org/10.1007/978-1-4419-1323-4
Décréau, P. M. E., Le Guirriec, E., Rauch, J. L., Trotignon, J. G., Canu, P., Darrouzet, F., et al. (2005). Density irregularities in the plasmasphere boundary layer: CLUSTER observations in the dusk sector. *Advances in Space Research*, *36*(10), 1964–1969. https://doi.org/10.1016/j.asr.2005.08.050
Frey, H. U., Haerendel, G., Mende, S. B., Forrester, W. T., Immel, T. J., & Ostgaard, N. (2004). Subauroral morning proton spots (SAMPS) as a result of plasmapause-ring-current interaction. *Journal of Geophysical Research*, *109*, A10305. https://doi.org/10.1029/2004JA010516
Gallagher, D. L., & Comfort, R. H. (2016). Unsolved problems in plasmasphere refilling. *Journal of Geophysical Research: Space Physics*, *121*, 1447–1451. https://doi.org/10.1002/2015JA022279
Khalipov, V. L., Stepanov, A. E., Kotova, G. A., & Bondar, E. D. (2016). Position variations of the polarization jet and injection boundary of energetic ions during substorms. *Geomagnetism and Aeronomy*, *56*(2), 174–180. https://doi.org/10.1134/S0016793216020080
Khazanov, G. (2011). *Kinetic theory of the inner magnetospheric plasma, Astrophysics and Space Science Library 372*. New York: Springer. https://doi.org/10.1007/978-1-4419-6797-8
Kotova, G. A., Bezrukikh, V. V., Verigin, M. I., Akentieva, O. S., & Smilauer, J. (2008). Study of notches in the Earth's plasmasphere based on data of the MAGION-5 satellite. *Cosmic Research*, *46*(1), 15–24. https://doi.org/10.1134/S0010952508010036
Kotova, G., Verigin, M., & Bezrukikh, V. (2014). The effect of the Earth's optical shadow on thermal plasma measurements in the plasmasphere. *Journal of Atmospheric and Solar: Terrestrial Physics*, *120*, 9–14. https://doi.org/10.1016/j.jastp.2014.08.013
Kotova, G., Verigin, M., & Bezrukikh, V. (2015). Physics-based reconstruction of the 3-D density distribution in the entire quiet time plasmasphere from measurements along a single pass of an orbiter. *Journal of Geophysical Research: Space Physics*, *120*, 7512–7521. https://doi.org/10.1002/2015JA021281
Kotova, G., Verigin, M., & Bezrukikh, V. (2017). Use of the physically based modeling to choose an adequate method for determining the plasmapause position. *Geomagnetism and Aeronomy*, *57*(4), 375–383. https://doi.org/10.1134/S0016793217040107
Lemaire, J. (1974). The 'Roche limit' of ionospheric plasma and the formation of the plasmapause. *Planetary and Space Science*, *22*(5), 757–766 . https://doi.org/10.1016/0032-0633(74)90145-7
Lemaire, J. (1976). Steady state plasmapause positions deduced from McIlwain's electric field models. *Journal of Atmospheric and Terrestrial Physics*, *38*(11), 1041–1046. https://doi.org/10.1016/0021-9169(76)90031-3
Lemaire, J. (1985). Formation and deformation of the plasmapause during a substorm event, in *Proceedings of the Conference on "Résultats du Projet Arcad 3 et des Programmes Récents en Physique de la Magnétosphere et de l'Ionosphere", Toulouse*, 22–25 mai, 976 pp., 239–260.
Lemaire, J., & Kowalkowski, L. (1981). The role of plasma interchange motion for the formation of a plasmapause. *Planetary and Space Science*, *29*(4), 469–478. https://doi.org/10.1016/0032-0633(81)90090-8
Lemaire, J. F., & Pierrard, V. (2008). Comparison between two theoretical mechanisms for the formation of the plasmapause and relevant observations. *Geomagnetism and Aeronomy*, *48*(5), 553–570. https://doi.org/10.1134/S0016793208050010
Lemaire, J., & Schunk, R. W. (1992). Plasmaspheric wind. *Journal of Atmospheric and Terrestrial Physics*, *54*(3-4), 467–477. https://doi.org/10.1016/0021-9169(92)90026-H
Lemaire, J., & Schunk, R. W. (1994). Plasmaspheric wind with non-closed streamlines. *Journal of Atmospheric and Terrestrial Physics*, *56*(12), 1629–1633. https://doi.org/10.1016/0021-9169(94)90092-2
Lemaire, J. F., Gringauz, K. I., with contributions from D. L. Carpenter, & Bassolo, V. (1998). *The Earth's Plasmasphere* (p. 350). Cambridge: Cambridge University Press.
Liu, W., Cao, J. B., Li, X., Sarris, T. E., Zong, Q.-G., Hartinger, M., et al. (2013). Poloidal ULF wave observed in the plasmasphere boundary layer. *Journal of Geophysical Research: Space Physics*, *118*, 4298–4307. https://doi.org/10.1002/jgra.50427
Mendillo, M., Baumgardner, J., & Wrote, J. (2016). SAR arcs we have seen: Evidence for variability in stable auroral red arcs. *Journal of Geophysical Research: Space Physics*, *121*, 245–262. https://doi.org/10.1002/2015JA021722
Moldwin, M. B., & Zou, S. (2012). The importance of the plasmasphere boundary layer for understanding inner magnetosphere dynamics. *Geophysical Monograph Series*, *199*, 321–327. https://doi.org/10.1029/2012GM001323
Murakami, G., Yoshioka, K., Yamazaki, A., Nishimura, Y., Yoshikawa, I., & Fujimoto, M. (2016). The plasmapause formation seen from meridian perspective by KAGUYA. *Journal of Geophysical Research: Space Physics*, *121*, 11,973–11,984. https://doi.org/10.1002/2016JA023377
Nishida, A. (1966). Formation of the plasmapause, or magnetospheric plasma knee, by a combined action of magnetospheric convection and plasma escape from the tail. *Journal of Geophysical Research*, *71*(23), 5669–5679. https://doi.org/10.1029/JZ071i023p05669
Park, C. G. (1973). Whistler observations of the depletion of the plasmasphere during a magnetospheric substorm. *Journal of Geophysical Research*, *78*(4), 672–683. https://doi.org/10.1029/JA078i004p00672
Pierrard, V., & Cabrera, J. (2006). Dynamical simulations of plasmapause deformations. *Space Science Reviews*, *122*(1-4), 119–126. https://doi.org/10.1007/s11214-005-5670-8
Pierrard, V., & Stegen, K. (2008). A three dimensional dynamic kinetic model of the plasmasphere. *Journal of Geophysical Research*, *113*, A10209. https://doi.org/10.1029/2008ja013060
Pierrard, V., & Voiculescu, M. (2011). The 3D model of the plasmasphere coupled to the ionosphere. *Geophysical Research Letters*, *38*, L12104. https://doi.org/10.1029/2011GL047767
Pierrard, V., Goldstein, J., André, N., Jordanova, V. K., Kotova, G. A., Lemaire, J. F., et al. (2009). Recent progress in physics-based models of the plasmasphere. *Space Science Reviews*, *145*(1-2), 193–229. https://doi.org/10.1007/s11214-008-9480-7
Tarcsai, G. (1985). Ionosphere-plasmasphere electron fluxes at middle latitudes obtained from whistlers. *Advances in Space Research*, *5*(4), 155–158. https://doi.org/10.1016/0273-1177(85)90131-0

Tsyganenko, N. A., & Sitnov, M. I. (2007). Magnetospheric configurations from a high-resolution data-based magnetic field model. *Journal of Geophysical Research*, *112*, A06225. https://doi.org/10.1029/2007JA012260

Verbanac, G., Pierrard, V., Bandic, M., Darrouzet, F., Rauch, J.-L., & Décréau, P. (2015). Relationship between plasmapause, solar wind and geomagnetic activity between 2007 and 2011 using Cluster data, Annales Geophysicae. *Annales de Geophysique*, *33*(10), 1271–1283. https://doi.org/10.5194/angeo-33-1271-2015